



OPEN

## Enhanced in situ H<sub>2</sub>O<sub>2</sub> production explains synergy between an LPMO with a cellulose-binding domain and a single-domain LPMO

Anton A. Stepnov, Vincent G. H. Eijsink & Zarah Forsberg

Lytic polysaccharide monooxygenases (LPMOs) are mono-copper enzymes that catalyze oxidative depolymerization of recalcitrant substrates such as chitin or cellulose. Recent work has shown that LPMOs catalyze fast peroxygenase reactions and that, under commonly used reaction set-ups, access to in situ generated H<sub>2</sub>O<sub>2</sub> likely limits catalysis. Based on a hypothesis that the impact of a cellulose-binding module (CBM) on LPMO activity could relate to changes in in situ H<sub>2</sub>O<sub>2</sub> production, we have assessed the interplay between CBM-containing ScLPMO10C and its truncated form comprising the catalytic domain only (ScLPMO10C<sub>TR</sub>). The results show that truncation of the linker and CBM leads to elevated H<sub>2</sub>O<sub>2</sub> production and decreased enzyme stability. Most interestingly, combining the two enzyme forms yields strong synergistic effects, which are due to the combination of high H<sub>2</sub>O<sub>2</sub> generation by ScLPMO10C<sub>TR</sub> and efficient productive use of H<sub>2</sub>O<sub>2</sub> by the full-length enzyme. Thus, cellulose degradation becomes faster, while enzyme inactivation due to off-pathway reactions with excess H<sub>2</sub>O<sub>2</sub> is reduced. These results underpin the complexity of ascorbic acid-driven LPMO reactions and reveal a potential mechanism for how LPMOs may interact synergistically during cellulose degradation.

Lytic polysaccharide monooxygenases (LPMOs) are monocopper enzymes that catalyze oxidative depolymerization of polysaccharide substrates, such as chitin<sup>1</sup>, cellulose<sup>2–4</sup> and xylan<sup>5–7</sup>. LPMOs depend on an electron source to maintain their catalytic cycle and possess a unique ability to act on crystalline surfaces of recalcitrant polysaccharides, making their targets prone to further degradation by classical hydrolytic enzymes<sup>8</sup>. The synergy between LPMOs, chitinases and cellulases has attracted significant attention not only in academia but also in industry<sup>1,9–14</sup>. Modern commercial cellulolytic cocktails, such as Cellic CTec2 and CTec3, benefit from the inclusion of LPMOs in their formulations<sup>10,15</sup>.

LPMOs were previously thought to use molecular oxygen as a co-substrate, but it has recently been shown that these enzymes prefer hydrogen peroxide, thus operating as peroxygenases rather than strict monooxygenases<sup>16</sup>. Importantly, due to the preference for H<sub>2</sub>O<sub>2</sub>, the rates of LPMO reactions that are carried out in the absence of exogenously added hydrogen peroxide are limited by in situ H<sub>2</sub>O<sub>2</sub> generation<sup>16–18</sup> and are low compared to reactions with controlled addition of H<sub>2</sub>O<sub>2</sub><sup>17,19,20</sup>.

Both non-enzymatic and enzyme-dependent pathways lead to hydrogen peroxide generation in typical LPMO reactions. Firstly, commonly used low-molecular-weight LPMO reductants, such as ascorbic acid, gallic acid and cysteine, are known to engage into direct reactions with dissolved molecular oxygen, yielding H<sub>2</sub>O<sub>2</sub><sup>21–23</sup>. Secondly, it is well established that reduced LPMOs have oxidase activity, which leads to hydrogen peroxide production<sup>24</sup> with rates that depend on the nature of the reductant that is being oxidized<sup>17,18,25</sup>. It is worth noting that, besides driving LPMO activity on carbohydrates, H<sub>2</sub>O<sub>2</sub> may promote auto-catalytic damage to the active site of the LPMO, especially when substrate concentrations are low<sup>16,26</sup>. All in all, a detailed understanding of the factors determining the rate of in situ H<sub>2</sub>O<sub>2</sub> generation in LPMO reactions is essential for unlocking the full potential of these enzymes.

One important but rather unexplored aspect of LPMO chemistry is the interplay between enzyme-dependent H<sub>2</sub>O<sub>2</sub> production and substrate binding. A few recent studies involving fungal (family AA9) and bacterial (family AA10) LPMOs have confirmed early suggestions by Kittl et al.<sup>24</sup> by showing that hydrogen peroxide generation by these enzymes is repressed in the presence of insoluble substrate<sup>27,28</sup>. Such observations make sense

Faculty of Chemistry, Biotechnology and Food Science, NMBU - Norwegian University of Life Sciences, 1432 Ås, Norway. email: vincent.eijsink@nmbu.no; zarah.forsberg@nmbu.no

considering the fact that binding to a crystalline surface will shield the active site from the solvent to a degree that will prevent the interaction of low-molecular reductants with the copper atom<sup>29</sup>. In Nature, binding of LPMOs to insoluble polysaccharides is often guided by carbohydrate-binding modules (CBMs)<sup>30</sup>. Compared to LPMO catalytic domains, CBMs are capable of stronger binding to substrates<sup>31,32</sup>, and it has been shown that CBMs have pronounced impact on LPMO activity and stability because they contribute to keeping the active site closer to the substrate<sup>32–34</sup>.

Considering the above, it is reasonable to assume that the presence or absence of a CBM will affect hydrogen peroxide production by LPMOs in reactions with insoluble polysaccharide substrates, with potential repercussions on (H<sub>2</sub>O<sub>2</sub>-driven) LPMO activity. To study these issues, we have used a CBM-containing family AA10 LPMO from *Streptomyces coelicolor* (ScLPMO10C) and its truncated form lacking the CBM and the linker (ScLPMO10C<sub>TR</sub>) as model bacterial enzymes and studied the interplay and possible synergy between these. We show that the two enzyme forms act synergistically during cellulose degradation and, by studying H<sub>2</sub>O<sub>2</sub> production and reductant depletion in various reaction set-ups, we show that this synergy relates to redox processes in the reaction mixture that affect co-substrate availability and oxidative enzyme inactivation. Next to shedding light on the possible interplay between CBM-containing and CBM-free LPMOs, our results provide fundamental insights into the complexity of LPMO reactions that are fueled by ascorbic acid, the most commonly used reductant in LPMO research.

## Results and discussion

**Protein production.** To investigate the impact of the cellulose-binding module (CBM) on LPMO performance in reactions with insoluble substrate, a well-characterized enzyme from the Gram-positive soil bacterium *Streptomyces coelicolor*, ScLPMO10C, was selected as the model. The LPMO and its truncated form lacking the linker and the CBM2, ScLPMO10C<sub>TR</sub> (Fig. 1A), were produced using previously described *E. coli* expression strains<sup>35</sup>. Both enzymes were isolated from the periplasm in soluble form and purified by ion-exchange and size-exclusion chromatography (Fig. 1B). The final yield amounted to approximately 60 mg of ScLPMO10C and 20 mg of ScLPMO10C<sub>TR</sub> per liter of culture.

### Hydrogen peroxide generation by ScLPMO10C and ScLPMO10C<sub>TR</sub> and assessment of free copper levels in the enzyme preparations.

In a recent study by our group, we showed that some of the previously published activity data for ScLPMO10C likely were affected by the presence of free copper in the reaction mixture, probably as a result of incomplete desalting of the enzyme preparations after copper-saturation<sup>28</sup>. It is well established that the combination of free Cu(II) ions and ascorbic acid will promote enzyme-independent H<sub>2</sub>O<sub>2</sub> generation<sup>21</sup>, sometimes referred to as reductant autooxidation, which will boost LPMO activity and affect enzyme stability<sup>28,36</sup>. To ensure that the residual free copper levels in ScLPMO10C and ScLPMO10C<sub>TR</sub> preparations used in the present study were minimal, protein-free samples were obtained from enzyme stock solutions by ultrafiltration through 3 kDa MWCO membranes. Analysis of these control samples with the HRP/Amplex Red assay, using 1 mM ascorbic acid as reductant, showed very low hydrogen peroxide production rates, compared to reactions with the LPMO (Fig. 2A), which demonstrates that the enzyme preparations contained negligible amounts of free copper.

Surprisingly, despite a comparable very low level of free copper in both enzyme preparations, as shown by the control reactions with the ultrafiltrates, the two enzyme variants (at 3 μM) showed a three-fold difference in the hydrogen peroxide generation rate (Fig. 2A). While it is reasonable to assume that these two enzymes generate different amounts of H<sub>2</sub>O<sub>2</sub> in the presence of cellulose, due to variation in substrate binding affinity (as discussed in detail below), we expected to see equal performance of both LPMOs under the conditions of the HRP/Amplex Red assay (i.e., in the absence of any polysaccharide substrate).

Given the fact that even very low amounts of free copper will lead to significant H<sub>2</sub>O<sub>2</sub> generation in this reaction set-up (Fig. 2B), one has to be extremely careful when interpreting the observed difference in H<sub>2</sub>O<sub>2</sub> production between ScLPMO10C and ScLPMO10C<sub>TR</sub>. Looking for explanations, we first considered the possibility that the difference is caused by differences in the rate by which trace amounts of free copper (e.g., 0.1 μM copper, see Fig. 2B) are released from the active site of the LPMOs due to different rates of auto-catalytic damage. Release of copper from the LPMO active site under reducing conditions is conceivable since it is known that auto-catalytic oxidation predominately affects copper-binding histidine residues<sup>16</sup>. Importantly, as demonstrated by the control experiment depicted in Fig. 2B, the gradual accumulation of free copper ions in solution would cause the apparent rate of hydrogen peroxide generation to change over time. Since the H<sub>2</sub>O<sub>2</sub>-production curves obtained for both LPMO variants (Fig. 2C) are linear, it seems safe to conclude that free copper does not contribute significantly to the generation of H<sub>2</sub>O<sub>2</sub> in this reaction set-up.

An additional control experiment with varying amounts of both LPMOs (0.5–3 μM) showed that the gap between the H<sub>2</sub>O<sub>2</sub>-generation rates is constant across all tested concentrations (Fig. 2D), which would not be the case if free copper is indeed released under the assay conditions at rates that differ between the two enzymes. Thus, it would seem that the observed difference in H<sub>2</sub>O<sub>2</sub> production between ScLPMO10C and ScLPMO10C<sub>TR</sub> relates to an intrinsic enzyme property, i.e., a difference in oxidase activity. A possible, although highly speculative, explanation is that the CBM weakly interacts with the substrate-binding surface of the catalytic domain, which could reduce oxidase activity by shielding the active site Cu(II) from the solvent and the reductant.

**Synergistic solubilization of cellulose by ScLPMO10C and ScLPMO10C<sub>TR</sub>.** Our next goal was to compare the performance of ScLPMO10C and ScLPMO10C<sub>TR</sub> during Avicel depolymerization. The hydrogen peroxide production gap between the full-length and truncated LPMO observed in the HRP/Amplex Red assay is likely to become more pronounced in the presence of cellulose. As alluded to above, existing data indicate that

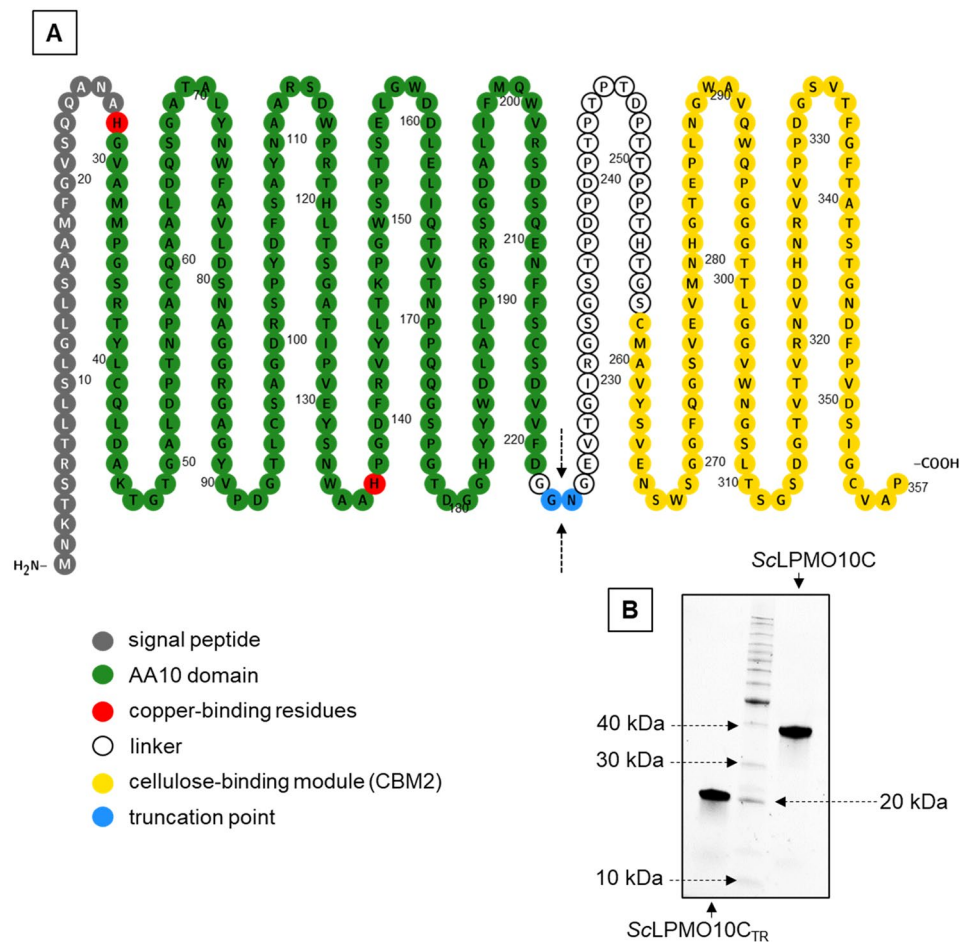


**Figure 1.** Domain architecture of ScLPMO10C (panel A) and SDS-PAGE of purified ScLPMO10C and ScLPMO10C<sub>TR</sub> (panel B). ScLPMO10C<sub>TR</sub> is a modified form of ScLPMO10C produced by truncation of the cellulose-binding module as indicated by the blue color and the arrows. For expression, the native signal peptide was replaced by the signal peptide of *Sm*LPMO10A (CBP21), which is shown in the figure. Domain boundaries were annotated using Pfam (<http://pfam.xfam.org/>), with minor manual adjustments based on inspection of the crystal structure of the catalytic domain (PDB: 4OY7) and the NMR structure of the cellulose-binding domain (PDB: 6F7E). The schematic representation of ScLPMO10C was created with the Protter protein visualization tool (<http://wlab.ethz.ch/protter>). See Fig. S1 for the uncropped and unprocessed gel image used to create panel B.

binding to polysaccharide substrates prevents LPMOs from producing hydrogen peroxide<sup>27,28</sup>. Furthermore, it is well established that the cellulose-binding module of ScLPMO10C is capable of much stronger interaction with substrate than the catalytic domain of the enzyme, and is thus important for keeping the enzyme active site closer to its substrate<sup>31,33</sup>. Hence, it is sensible to expect enhanced in situ hydrogen peroxide generation by weak-binding ScLPMO10C<sub>TR</sub> compared to the stronger binding full-length LPMO during Avicel degradation.

Interestingly, if one accepts the premise that LPMO action is limited by access to H<sub>2</sub>O<sub>2</sub>, and if the above considerations about expected H<sub>2</sub>O<sub>2</sub> production levels in the presence of substrate are true, it is conceivable that weak binding ScLPMO10C<sub>TR</sub> and stronger binding full-length ScLPMO10C may act synergistically during Avicel degradation. The truncated LPMO will spend most of its time in solution, generating hydrogen peroxide to boost the oxidative activity of the wild-type enzyme that is anchored on a crystalline surface by its CBM. On the other hand, the truncated enzyme, which is prone to damaging off-pathway reactions<sup>33</sup>, may be protected by the full-length enzyme that removes H<sub>2</sub>O<sub>2</sub> from the solution in productive reactions. To test this hypothesis, we carried out Avicel degradation experiments with ScLPMO10C, ScLPMO10C<sub>TR</sub> or a combination of both LPMOs in the presence of ascorbic acid (Fig. 3).

Cellulose depolymerization by 1 or 2 μM ScLPMO10C resulted in a slow (0.05 min<sup>-1</sup>) but steady release of oxidized products over 24 h. Such low catalytic rates are common among bacterial LPMOs operating in the absence of exogenously added hydrogen peroxide<sup>1,18,28</sup>. In contrast to the full-length enzyme, the reactions with 1 or 2 μM ScLPMO10C<sub>TR</sub> were much (approximately fourfold) faster. In these reactions, product release diminished early during the course of the experiment. This is indicative of LPMO auto-catalytic inactivation. It is well

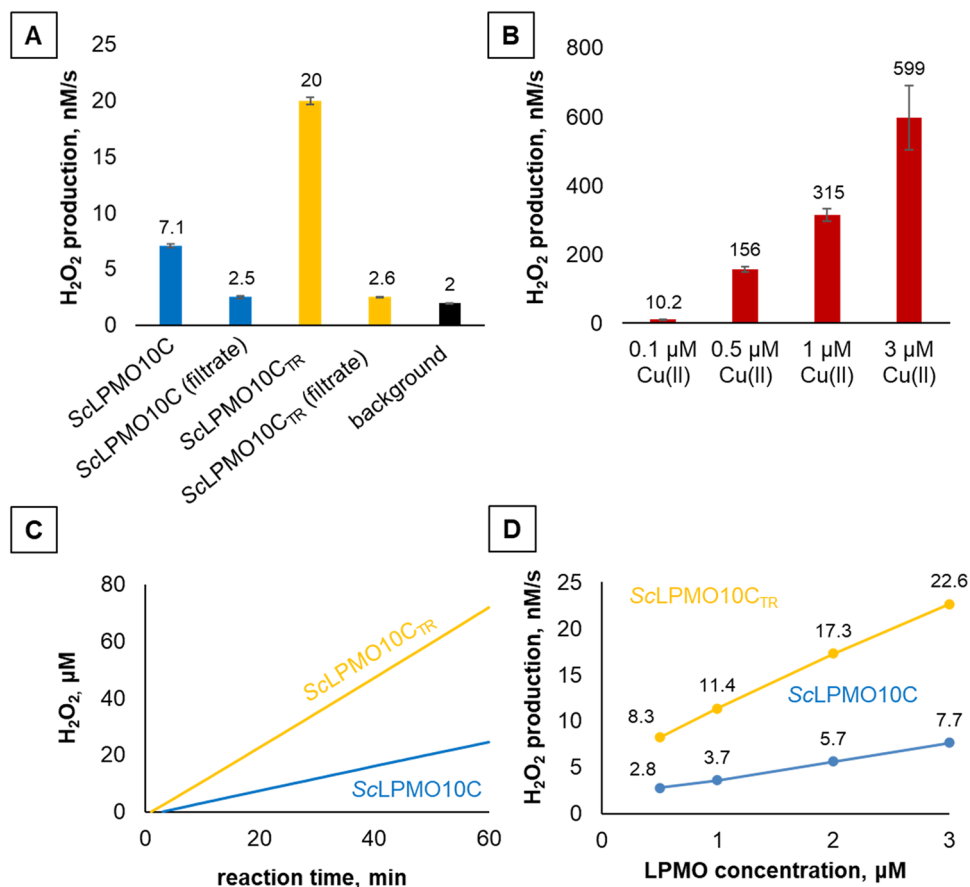


**Figure 2.** Apparent hydrogen peroxide production in reactions containing ScLPMO10C and ScLPMO10C<sub>TR</sub> (panels A, C, D) or Cu(II)SO<sub>4</sub> (panel B). All experiments were carried out using 1 mM ascorbic acid in 50 mM sodium phosphate buffer, pH 6.0, at 30 °C. Reaction mixtures contained 5 U/ml HRP, 100 μM Amplex Red, 1% (v/v) DMSO and varying concentrations of LPMOs and Cu(II)SO<sub>4</sub>. The data shown in panels A and C are for LPMO concentrations of 3 μM. H<sub>2</sub>O<sub>2</sub> production rates were derived from linear progress curves (such as shown in panel C; in this experiment the signal is monitored continuously). Free copper control experiments designated as “ScLPMO10C filtrate” and “ScLPMO10C<sub>TR</sub> filtrate” in panel A were carried out using protein-free samples obtained from enzyme stock solutions by ultrafiltration. Such filtrates will contain the same amount of free copper ions as the LPMO preparations. The black bar in panel A denotes the background rate of hydrogen peroxide accumulation in the reaction containing reductant but lacking LPMO. Error bars indicate standard deviations between triplicates. The rates shown in panels A and D were obtained in independent experiments. Error bars in panel D are hidden behind the markers.

known that LPMO instability is promoted by reduced binding to the substrate<sup>37</sup> and high levels of H<sub>2</sub>O<sub>2</sub><sup>16</sup>, and both apply to ScLPMO10C<sub>TR</sub> relative to the full-length enzyme.

Strikingly, reactions with 1 μM ScLPMO10C + 1 μM ScLPMO10C<sub>TR</sub> or 1 μM ScLPMO10C + 2 μM ScLPMO10C<sub>TR</sub> did not show signs of enzyme inactivation and generated higher product levels compared to reactions with the individual LPMOs (Fig. 3). The amount of oxidized products released after 24 h was 1.3-fold (1 μM ScLPMO10C + 1 μM ScLPMO10C<sub>TR</sub>) and 2.6-fold (1 μM ScLPMO10C + 2 μM ScLPMO10C<sub>TR</sub>) higher compared to the sum of the products generated by these enzymes in individual reactions, indicative of a synergistic action. The reaction with 1 μM ScLPMO10C + 2 μM ScLPMO10C<sub>TR</sub> is remarkable, showing a much higher rate than ScLPMO10C alone, no signs of enzyme inactivation and high product levels. Considering the observed (Fig. 2) and expected H<sub>2</sub>O<sub>2</sub> production levels, the increased rate of the reaction may be explained by increased levels of available H<sub>2</sub>O<sub>2</sub>, which is produced by the truncated enzyme. At the same time, the truncated enzyme is protected from damaging off-pathway reactions with H<sub>2</sub>O<sub>2</sub> because the oxidant is used in productive reactions by the full-length enzyme. There are indications, from modelling<sup>38</sup> and experiments<sup>39</sup>, that binding of H<sub>2</sub>O<sub>2</sub> by an LPMO is promoted by the presence of substrate. Thus, it is plausible that the full-length enzyme, with high substrate affinity, outcompetes the truncated enzyme, with low substrate affinity, for binding (and reacting with) H<sub>2</sub>O<sub>2</sub>.

Paradoxically, the initial rate of the most efficient reaction (1 μM ScLPMO10C + 2 μM ScLPMO10C<sub>TR</sub>) was still considerably lower than the initial rate of the reaction with 1 μM or 2 μM ScLPMO10C<sub>TR</sub> alone (Fig. 3, first three hours). Looking for possible explanations, it is important to take into account the expected instability of ScLPMO10C<sub>TR</sub>, which may lead to gradual release of copper into solution, which will boost the activity of still intact LPMOs because free copper promotes LPMO-independent H<sub>2</sub>O<sub>2</sub> generation in the presence of ascorbic

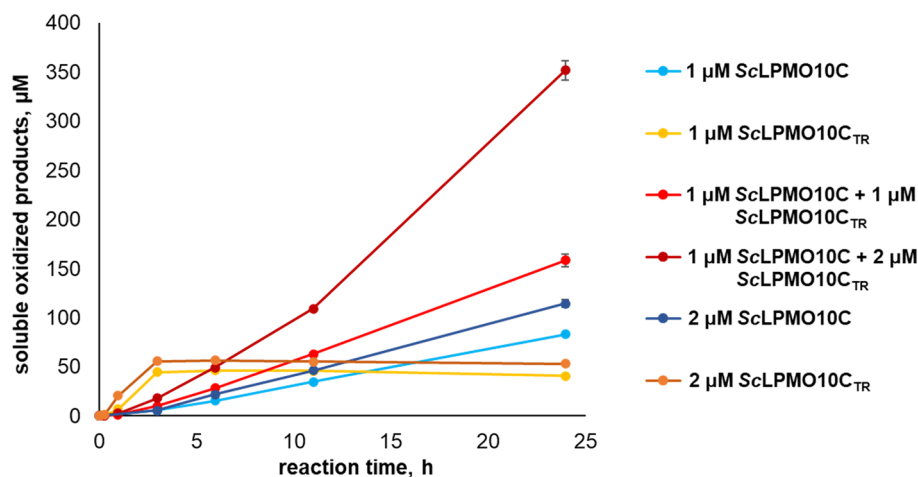


**Figure 3.** Cellulose oxidation by ScLPMO10C and ScLPMO10C<sub>TR</sub>. The graph shows soluble oxidized products released from 1% (w/v) Avicel by ScLPMO10C, ScLPMO10C<sub>TR</sub> or mixtures of these LPMOs in the presence of 1 mM ascorbic acid. The reactions were carried out in 50 mM sodium phosphate buffer, pH 6.0, supplied with 1 mM ascorbic acid, at 30 °C. Error bars indicate standard deviations between triplicates.

acid (Fig. 2B). In other words, the decreased initial rate of product release observed upon adding ScLPMO10C to a reaction with ScLPMO10C<sub>TR</sub>, may be a direct consequence of the above-mentioned stabilization of the truncated enzyme. This complicated scenario is further explained and experimentally verified below.

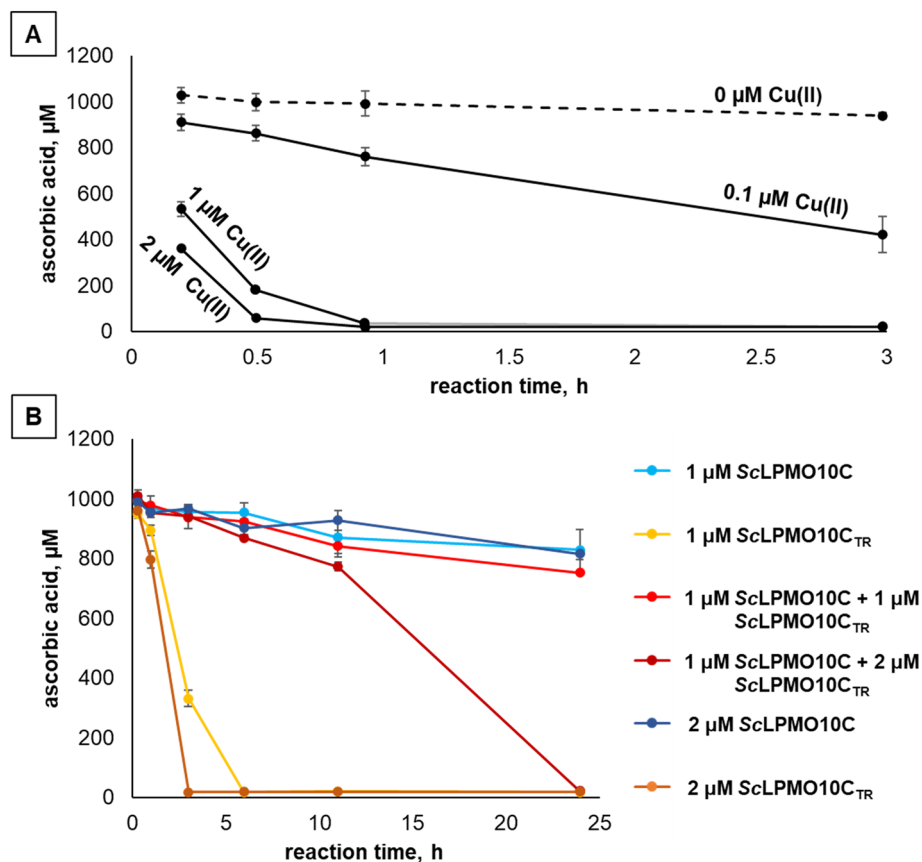
**Reductant consumption in reactions with ScLPMO10C and ScLPMO10C<sub>TR</sub>.** If copper is indeed released from the active site of unstable LPMOs then this effect should be carefully accounted for while interpreting the data shown on Fig. 3. Thus, our next goal was to evaluate whether spectroscopic quantification of ascorbic acid in LPMO reactions can be used as a tool to detect leakage of copper ions from the oxidatively damaged histidine brace. At standard aerobic conditions, the depletion of reductant is driven by LPMO-dependent H<sub>2</sub>O<sub>2</sub> production (oxidase activity), LPMO-dependent substrate oxidation (peroxygenase activity), reactions between hydrogen peroxide and ascorbic acid<sup>25</sup> and enzyme-independent H<sub>2</sub>O<sub>2</sub> generation (i.e., oxidation of the reductant by O<sub>2</sub>). For some reductants, including ascorbic acid, enzyme-independent H<sub>2</sub>O<sub>2</sub> generation is strongly promoted by free copper<sup>28</sup>. Indeed, under the reaction conditions used here, major effects of free copper will occur at concentrations (e.g., 0.1 µM; (Fig. 2B) that are well below the LPMO concentrations (1–3 µM) used in this study. Thus, copper release caused by oxidative damage to the active site of only a fraction of the LPMOs could strongly affect the activity (and exposure to H<sub>2</sub>O<sub>2</sub>) of the remaining intact enzymes.

Figure 4A shows the impact of free copper on reductant depletion under the conditions used for the reactions shown in Figs. 2 and 3. In accordance with Fig. 2B, showing increased H<sub>2</sub>O<sub>2</sub> production upon addition of 0.1 µM Cu(II), Fig. 4A shows that the presence of 0.1 µM Cu(II) drastically speeds up the turnover of ascorbic acid. Thus, there is no doubt that under the conditions used here, which are often applied in the field, release of copper from damaged LPMOs will lead to increased H<sub>2</sub>O<sub>2</sub> production and, thus, fueling of the remaining intact LPMOs.

Quantification of ascorbic acid in reactions with substrate (i.e., the reactions displayed in Fig. 3) revealed slow and steady reductant depletion in the reactions with 1 µM ScLPMO10C, 2 µM ScLPMO10C or 1 µM ScLPMO10C + ScLPMO10C<sub>TR</sub> (Fig. 4B), which coincides with the close to linear product formation progress curves of Fig. 3. In stark contrast, the reactions with 1 or 2 µM ScLPMO10C<sub>TR</sub> showed rapid and complete ascorbic acid consumption within first 6 or 3 h of the experiment, respectively (Fig. 4B). Notably, this high consumption is nowhere near to being proportional to the low amounts of oxidized LPMO products released in these reactions (Fig. 3), showing that reducing power is used in another process, for example reduction of O<sub>2</sub> to H<sub>2</sub>O<sub>2</sub>. The reductant depletion rates observed with 1 or 2 µM ScLPMO10C<sub>TR</sub> are comparable to the results of the control experiments with free Cu(II) (Fig. 4A) and strongly suggest that copper indeed leaves the LPMO active site, which will increase H<sub>2</sub>O<sub>2</sub> production in the presence of ascorbic acid.

Thus, we propose, that the high initial rate and fast enzyme inactivation observed in reactions with 1 or 2 µM ScLPMO10C<sub>TR</sub> (Fig. 3) are the result of a self-reinforcing process: The LPMO binds weakly to the substrate and produces lots of H<sub>2</sub>O<sub>2</sub>; this leads to higher LPMO activity and higher LPMO inactivation, where the latter leads to the release of free copper, which, by promoting H<sub>2</sub>O<sub>2</sub> production, further increases LPMO activity and LPMO inactivation. The result is a high initial rate of reaction and fast cessation of the reaction, in accordance with the progress curves shown in Fig. 3. This self-reinforcing process will be hindered upon addition of the full-length LPMO that uses the H<sub>2</sub>O<sub>2</sub> in productive LPMO reactions, which explains the paradox drawn up in the previous section.

It may seem contradictory that, even in the presence of substrate, ScLPMO10C<sub>TR</sub> shows signs of inactivation (reflected in excessive ascorbic acid consumption) within 1 h of the reaction (Fig. 4B), whereas this enzyme gave a linear H<sub>2</sub>O<sub>2</sub> production curve in the experiment depicted in Fig. 2C. Importantly, in this latter experiment,



**Figure 4.** Ascorbic acid consumption in reactions containing  $\text{Cu(II)SO}_4$  (panel A) or LPMOs (panel B). The reactions were carried out at 30 °C in 50 mM sodium phosphate buffer, pH 6.0, supplied with 1% (w/v) Avicel, and were initiated by the addition of 1 mM ascorbic acid at  $t=0$ . The reductant concentration was determined by UV spectroscopy immediately after removing the insoluble LPMO substrate by filtration. Note that the reductant depletion curves in panel B were obtained using the same samples as shown in Fig. 3. Error bars indicate standard deviations between triplicates.

generated  $\text{H}_2\text{O}_2$  is rapidly consumed by the HRP present in the reaction, which will drastically reduce enzyme inactivation and the consequent release of copper that promotes reductant consumption.

Importantly, while cessation of product formation in LPMO reactions is usually ascribed to enzyme inactivation, the data in Fig. 4 illustrate, that, due to the self-reinforcing nature of the LPMO inactivation process, fast depletion of ascorbic acid may occur, which will also stop the LPMO reaction. In the reactions shown here, both factors may have played a role. However, the progress curves for the reaction with 1 μM ScLPMO10C<sub>TR</sub> indicate that product formation stopped at or before 3 h (Fig. 3), while the reductant had not yet been completely depleted (Fig. 4B). Hence, in this experiment, oxidative inactivation of the LPMO was the dominating process leading to cessation of the reaction.

More insight into this matter may be derived from the ascorbic acid depletion curve for the reaction with 1 μM ScLPMO10C + 2 μM ScLPMO10C<sub>TR</sub>, which displayed an apparent biphasic behavior (Fig. 4B). A slow (i.e., enzyme-dependent) reductant consumption phase was followed by a phase with a faster decrease in the ascorbic acid concentration. Expansion of the progress curves shown in Figs. 3 and 4 with additional data points confirmed the biphasic nature of the process. Figure 5 shows that the phase with steady ascorbic acid consumption was followed by a phase of rapid reductant consumption and cessation of product formation that reflects a collapse of the reaction system, similar to what was seen for the reactions with ScLPMO10C<sub>TR</sub> only, where this collapse happened earlier during the reaction due to the absence of the  $\text{H}_2\text{O}_2$ -consuming full-length enzyme (Fig. 4B).

The only plausible explanation for the collapse observed in this biphasic reaction is the release of copper by damaged LPMOs. Under turnover conditions gradual LPMO inactivation and copper-release from damaged LPMOs are to be expected due to off-pathway reactions, even though, in well controlled reaction systems, off-pathway reactions may be infrequent and not necessarily always destructive for the LPMO<sup>40</sup>. It is conceivable that at about 15 h in the biphasic reaction accumulated copper reached levels that triggered the self-reinforcing enzyme inactivation process described above. This process could initially speed up the reaction rate (as is visible in Fig. 5, showing a vaguely sigmoidal curve for product formation) but will lead to system collapse and rapid ascorbic acid depletion. Product formation (Fig. 3) and ascorbic acid depletion (Fig. 4B) remained constant

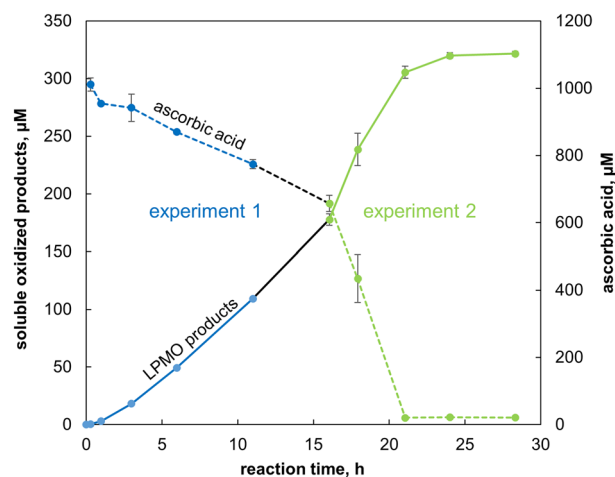


**Figure 5.** Release of oxidized products and reductant depletion in the reaction with  $1 \mu\text{M ScLPMO10C} + 2 \mu\text{M ScLPMO10C}_{\text{TR}}$ . The reactions were carried out at  $30^\circ\text{C}$  in  $50 \text{ mM}$  sodium phosphate buffer,  $\text{pH } 6.0$ , supplied with  $1\%$  (w/v) Avicel and were initiated by adding  $1 \text{ mM}$  ascorbic acid. The data shown in blue and green color represent two independent experiments. The blue progress curves (“experiment 1”) are the same as shown in Figs. 3 and 4B. In the second identical experiment (green) only later time points were monitored. The black lines connect the blue curves with the green curves. The reductant concentration was determined by UV spectroscopy immediately after removing the insoluble LPMO substrate by filtration. Error bars indicate standard deviations for triplicates.

for the full 24 h of the reaction containing 50% less of the truncated LPMO ( $1 \mu\text{M ScLPMO10C} + 1 \mu\text{M ScLPMO10C}_{\text{TR}}$  reaction). So, in this reaction, where one would expect less  $\text{H}_2\text{O}_2$  production and less enzyme inactivation, the turning point leading to rapid ascorbic acid depletion and biphasic behavior was never reached because there was less release of free copper into solution.

**Stability of ScLPMO10C and ScLPMO10C<sub>TR</sub> in the absence of substrate.** In line with previously published data, the above is based on the assumption that inactivation of an LPMO in the absence of substrate will relate to the oxidase activity of that LPMO (i.e.,  $\text{H}_2\text{O}_2$  production). To verify this assumption, we assessed the stability of the full-length and truncated enzymes under reducing conditions in the absence of substrate.  $2 \mu\text{M ScLPMO10C}$  or  $2 \mu\text{M ScLPMO10C}_{\text{TR}}$  were pre-incubated with  $1 \text{ mM}$  ascorbic acid for 2 h to promote inactivation. Aliquots were taken at various time points and then supplied with Avicel and another (the same) dose of ascorbic acid to assess the residual activity. This approach is not without limitations because free copper ions that have left the histidine brace as a result of enzyme inactivation will affect the subsequent LPMO reaction with Avicel where free copper will affect both activity and stability. Nevertheless, the results, depicted in Fig. 6, show a clear difference: the full-length LPMO retained most of its catalytic potential during the pre-incubation, whereas the truncated enzyme was rapidly inactivated. This difference is expected in light of the difference in  $\text{H}_2\text{O}_2$  production by the two enzymes (Fig. 2A). Taken together, the results shown in Figs. 2 and 6 suggest that truncation of the CBM significantly impairs the oxidative stability of ScLPMO10C in the absence of substrate, which is remarkable.

**Concluding remarks.** This study provides insight into the interplay between LPMOs with different  $\text{H}_2\text{O}_2$  generation and consumption capabilities. Being a much better hydrogen peroxide producer, ScLPMO10C<sub>TR</sub> is able to enhance cellulose oxidation by ScLPMO10C. At the same time, ScLPMO10C protects ScLPMO10C<sub>TR</sub> from fast auto-catalytic inactivation by removing excess  $\text{H}_2\text{O}_2$ . The synergistic action of the two LPMOs allowed for steady cellulose depolymerization over 24 h, with an efficiency that clearly surpassed the efficiencies of the individual enzymes.

While these results shed light on the complexity of LPMO reactions, especially when using “copper-sensitive” reductants, it remains to be seen whether the synergy observed here also occurs in Nature. LPMOs are abundant and many organisms contain multiple LPMOs, some with and some without CBMs. These CBM-free LPMOs could help fueling other LPMOs with  $\text{H}_2\text{O}_2$  as shown above, and could also fuel other  $\text{H}_2\text{O}_2$ -dependent enzymes such as lignin peroxidases<sup>41</sup>. On the other hand, in contrast to the catalytic domain of CBM-containing ScLPMO10C, these natural single domain LPMOs may very well have evolved to bind their substrates strongly, as observed for, e.g., the archetypal single domain LPMO *SmLPMO10A* (or CBP21;<sup>39</sup>), and may thus be less efficient  $\text{H}_2\text{O}_2$ -producers.

While we expected relatively fast  $\text{H}_2\text{O}_2$  generation by ScLPMO10C<sub>TR</sub> in reactions with cellulose because of low binding, the truncated LPMO was found to produce more hydrogen peroxide than the full-length enzyme even in the absence of substrate. As we show and discuss above, this surprising result is not driven by free copper and thus seems related to hitherto unknown effects of the CBM on LPMO oxidase activity. It is possible that the

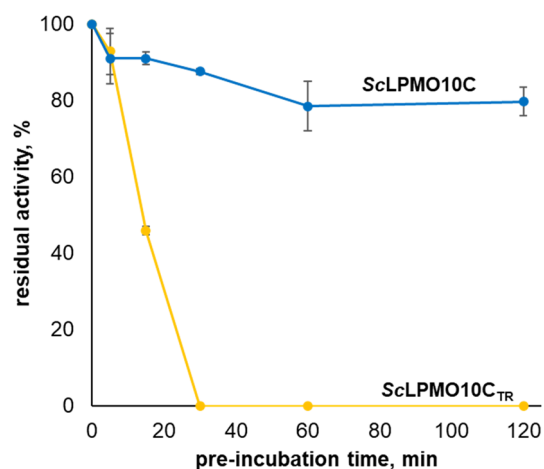


**Figure 6.** Oxidative stability of ScLPMO10C and ScLPMO10C<sub>TR</sub>. The figure shows the residual activity of 1  $\mu$ M ScLPMO10C and 1  $\mu$ M ScLPMO10C<sub>TR</sub> in a reaction with 1% (w/v) Avicel after various periods of pre-incubation with 1 mM ascorbic acid in the absence of substrate (i.e., under conditions that promote auto-catalytic inactivation). The cellulose degradation reaction was carried out for 24 h at 30 °C in 50 mM sodium phosphate buffer, pH 6.0, supplied with fresh 1 mM ascorbic acid. Error bars indicate standard deviations between triplicates.

higher H<sub>2</sub>O<sub>2</sub> production rate of ScLPMO10C<sub>TR</sub> in the absence of substrate is an artifact of LPMO truncation, which, in principle could lead to minor changes in the enzyme structure that could make the reduced copper more prone to oxidation by O<sub>2</sub>. However, this seems unlikely, given the fact that the truncation point is > 35 Å away from the active site and that the X-ray structure of ScLPMO10C<sub>TR</sub> shows no anomalies<sup>35</sup> (PDB: 4OY7). Another possible explanation is that the catalytic and cellulose-binding domains of ScLPMO10C interact in an inter-molecular or intra-molecular fashion. It is tempting, although highly speculative, to propose that the CBM may protect the LPMO from auto-catalytic damage in the absence of substrate by shielding the active site from the reductant (preventing reduction), or from reacting with O<sub>2</sub>, thus keeping the fraction of H<sub>2</sub>O<sub>2</sub>-producing enzyme molecules low. Further studies are needed to explore this scenario.

In addition to providing insights into the possible impact of CBMs on LPMO functionality and generating more insight into the crucial role of H<sub>2</sub>O<sub>2</sub> in LPMO catalysis, the present data shed light on the complexity of interpreting ascorbic acid-driven LPMO reactions. Ascorbic acid was, somewhat fortuitously, used in research leading to the discovery of LPMO activity<sup>1</sup> and has been used by many researchers since. This “copper-sensitive” reductant may engage in multiple reactions that are difficult to control and assess. One of these reactions, the scavenging of excess H<sub>2</sub>O<sub>2</sub> (i.e., further reduction to water) was not considered in the above because there is ample data showing that this reaction is slow relative to the other possible reactions<sup>17,40</sup>.

Progress curves for LPMO reactions with ascorbic acid often show apparent enzyme inactivation and the present study reveals, to the best of our knowledge for the first time, a plausible underlying mechanism. We show that release of copper ions as a consequence of (well known;<sup>16,37</sup>) oxidative damage to the LPMO active site triggers a self-reinforcing chain reaction leading to increased enzyme-independent H<sub>2</sub>O<sub>2</sub> generation, rapid enzyme inactivation and reductant depletion. Similar processes may occur in reactions with other reductants whose ability to reduce O<sub>2</sub> is copper-dependent, such as L-cysteine<sup>23</sup> and reduced glutathione<sup>42</sup>. While fully controlling and understanding all these processes remains challenging, the present study underpins that optimization of LPMO activity and stability requires control of H<sub>2</sub>O<sub>2</sub> levels and that, in many commonly used experimental settings, these levels are affected not only by LPMO oxidase activity but also by LPMO inactivation. Since oxidase activity varies between LPMOs<sup>17,43</sup> optimal conditions for LPMO reactions, and the relative impact of free copper, will vary.

## Methods

**Materials.** Chemicals were obtained from Sigma-Aldrich (St. Louis, MO, USA) unless specified otherwise. The model microcrystalline cellulose substrate used in the study was Avicel PH-101 with particle size of approximately 50  $\mu$ m. 100 mM ascorbic acid stock solutions were prepared in metal-free TraceSELECT water (Honeywell, Charlotte, NC, USA) and then filter-sterilized using 0.22  $\mu$ m syringe filters. Amplex Red was purchased from Thermo Fisher Scientific (Waltham, MA, USA) and dissolved in DMSO at 10 mM final concentration. The reductant and Amplex Red solutions were aliquoted, stored at -20 °C in light-protected tubes and used only once after thawing. Horseradish peroxidase type II (HRP; Sigma-Aldrich, St. Louis, MO, USA) was kept at 100 U/ml concentration in 50 mM sodium phosphate buffer, pH 6.0 at 4 °C. Tryptone and yeast extract were obtained from Thermo Fisher Scientific.

**Protein production and purification.** Previously generated ScLPMO10C and ScLPMO10C<sub>TR</sub> expressing *E. coli* BL21 DE3 strains<sup>35</sup> were used to inoculate Terrific Broth (TB) medium supplied with 100  $\mu$ g/ml ampicil-



lin. The cultures (2 × 500 ml for each LPMO-expressing strain) were incubated for 24 h at 30 °C in a LEX-24 Bioreactor (Harbinger Biotechnology & Engineering, Markham, Canada) using compressed air for aeration. The cells were harvested by centrifugation (6000 × g for 10 min at 4 °C) using a Beckman Coulter centrifuge (Brea, CA, USA). Periplasmic extracts were produced by applying osmotic shock as described previously<sup>44</sup> and were filter-sterilized through 0.22-µm syringe filters prior to further purification. These extracts were then subjected to ion-exchange chromatography using HiTrap Q FF (Q Sepharose) 5-ml columns (GE Healthcare, Chicago, USA). Proteins were eluted at 2.5 ml/min flow rate with a linear gradient of NaCl (0–500 mM, 250 ml) in the starting buffer (50 mM Tris-HCl, pH 7.5). LPMO-containing fractions were pooled, concentrated to approximately 1 ml volume (Vivaspin ultrafiltration tubes, 10 kDa MWCO, Sartorius, Göttingen, Germany) and loaded onto a ProteoSEC Dynamic 16/60 3–70 HR preparative size-exclusion column (Protein Ark, Sheffield, UK) operating at 1 ml/min flow rate and equilibrated with 50 mM Tris-HCl, pH 7.5, containing 200 mM NaCl. Purity of resulting ScLPMO10C and ScLPMO10C<sub>TR</sub> preparations was confirmed by SDS-PAGE. The LPMO concentration was determined using UV spectroscopy at 280 nm. The theoretical extinction coefficients were predicted using the Expasy ProtParam tool<sup>45</sup>.

**Copper saturation.** Purified LPMO solutions were concentrated to 0.5 ml volume using Vivaspin ultrafiltration tubes (10 kDa MWCO, Sartorius, Göttingen, Germany) and incubated with two-fold molar surplus of Cu(II)SO<sub>4</sub> at room temperature for 30 min. The excess (unbound) copper was removed by desalting with a PD MidiTrap G-25 gravity flow column (GE Healthcare, Chicago, USA), equilibrated with 50 mM sodium phosphate buffer, pH 6.0. To ensure effective free copper removal, the ScLPMO10C and ScLPMO10C<sub>TR</sub> samples were then subjected to multiple consecutive rounds of dilution and concentration using 50 mM sodium phosphate buffer, pH 6.0 and Vivaspin ultrafiltration tubes. The resulting total dilution factors for solutions of copper-saturated LPMOs amounted to at least 160 000.

**Hydrogen peroxide detection.** In situ hydrogen peroxide generation in LPMO reactions was assessed using a modified HRP/Amplex Red assay protocol<sup>18</sup>, originally proposed by Kittl et al.<sup>24</sup>. In brief, 90 µl of LPMO solution in 50 mM sodium phosphate buffer, pH 6.0, supplied with HRP and Amplex Red, was pre-incubated for 5 min at 30 °C in a 96-well microtiter plate. Next, 10 µl of 10 mM ascorbic acid was added to start the reaction, followed by 10 s of mixing at 600 RPM inside a Varioscan LUX plate reader (Thermo Fisher Scientific, Waltham, MA, USA). Hydrogen peroxide was detected by monitoring the formation of resorufin at 563 nm. The final concentrations of LPMOs, HRP, Amplex Red and ascorbic acid were 0.5–3 µM, 5 U/ml, 100 µM and 1 mM, respectively. H<sub>2</sub>O<sub>2</sub> standard solutions were prepared in 50 mM sodium phosphate buffer, pH 6.0, and supplied with 1 mM ascorbic acid prior to the addition of HRP and Amplex Red. The background non-enzymatic H<sub>2</sub>O<sub>2</sub> production was assessed in a control experiment with 1 mM ascorbic acid and no LPMO.

To ensure that the observed LPMO-dependent hydrogen peroxide generation is not biased by residual free copper ions in enzyme preparations, protein-free samples were obtained from the LPMO stock solutions using 3 kDa MWCO 1.5 ml ultrafiltration tubes (VWR International, Radnor, PA, USA) and were used to set up control experiments by substituting LPMOs with the same amount of filtrates, as previously described<sup>28</sup>.

**LPMO reactions with microcrystalline cellulose.** LPMO reactions with insoluble substrate (1% w/v Avicel) were carried out in 50 mM sodium-phosphate buffer, pH 6.0 using an Eppendorf thermomixer (Eppendorf, Hamburg, Germany) set to 30 °C and 950 RPM. The reactions were started by supplying 1 mM ascorbic acid (final concentration).

Aliquots were taken at various time points, and the reactions were quenched by removing the insoluble substrate using a 96-well filter plate (Millipore, Burlington, MA, USA). The concentration of ascorbic acid in filtered solutions was determined by UV spectrometry at 255 nm wavelength. Standard solutions of the reductant were prepared in metal-free TraceSELECT water. The samples were then treated with 2 µM of recombinant *Thermobifida fusca* GH6 endoglucanase (*TfCel6A*; produced in-house)<sup>46</sup> at 37 °C overnight to convert soluble C1-oxidized oligosaccharides to a simple mixture of oxidized dimers and trimers (i.e. GlcGlc1A and Glc<sub>2</sub>Glc1A).

**LPMO oxidative stability assay.** The oxidative stability of ScLPMO10C and ScLPMO10C<sub>TR</sub> was assessed by pre-incubating 2 µM enzyme in 50 mM sodium phosphate buffer, pH 6.0, containing 1 mM ascorbic acid, for two hours at 30 °C. Aliquots were taken at various time points and supplied with 1% (w/v) Avicel and another (the same) dose of ascorbic acid. LPMO reactions with Avicel were carried out for 24 h and then stopped by filtering out the insoluble substrate. These samples were treated with *TfCel6A* as described above and used to quantify the residual LPMO activity. The final concentration of both LPMOs in the reactions with Avicel was 1 µM.

**Quantification of LPMO products.** C1-oxidized soluble LPMO products were detected and quantified by high-performance anion-exchange chromatography with pulsed amperometric detection (HPAEC-PAD) using a Dionex ICS6000 system (Thermo Scientific, San Jose, CA, USA) equipped with a CarboPac PA200 analytical column, as recently described<sup>47</sup>. In brief, a concave gradient from 1 to 100 mM potassium methanesulfonate (KMSA) was applied over 14 min with 63 µl/min flow rate to separate native and C1-oxidized oligosaccharides, followed by a 3 min washing step (100 mM KMSA) and a 9 min column reconditioning step (1 mM KMSA). LPMO products were quantified using standard mixtures of C1-oxidized cellobiose and cellobiose, which were produced in-house using cellobiose dehydrogenase<sup>48</sup>, according to a previously published protocol<sup>49</sup>.

## Data availability

The data that support the findings of this study are available in Figs. 1–6.

Received: 22 February 2022; Accepted: 29 March 2022

Published online: 12 April 2022

## References

1. Vaaje-Kolstad, G. *et al.* An oxidative enzyme boosting the enzymatic conversion of recalcitrant polysaccharides. *Science* **330**, 219–222 (2010).
2. Forsberg, Z. *et al.* Cleavage of cellulose by a CBM33 protein. *Protein Sci.* **20**, 1479–1483 (2011).
3. Quinlan, R. J. *et al.* Insights into the oxidative degradation of cellulose by a copper metalloenzyme that exploits biomass components. *Proc. Natl. Acad. Sci. U.S.A.* **108**, 15079–15084 (2011).
4. Phillips, C. M., Beeson, W. T., Cate, J. H. & Marletta, M. A. Cellobiose dehydrogenase and a copper-dependent polysaccharide monooxygenase potentiate cellulose degradation by *Neurospora crassa*. *ACS Chem. Biol.* **6**, 1399–1406 (2011).
5. Couturier, M. *et al.* Lytic xylan oxidases from wood-decay fungi unlock biomass degradation. *Nat. Chem. Biol.* **14**, 306–310 (2018).
6. Frommhagen, M. *et al.* Discovery of the combined oxidative cleavage of plant xylan and cellulose by a new fungal polysaccharide monooxygenase. *Biotechnol. Biofuels.* **8**, 101 (2015).
7. Hegnar, O. A. *et al.* Quantifying oxidation of cellulose-associated glucuronoxylan by two lytic polysaccharide monooxygenases from *Neurospora crassa*. *Appl. Environ. Microbiol.* **87**, e0165221 (2021).
8. Eibinger, M. *et al.* Cellulose surface degradation by a lytic polysaccharide monooxygenase and its effect on cellulase hydrolytic efficiency. *J. Biol. Chem.* **289**, 35929–35938 (2014).
9. Dimarogona, M., Topakas, E., Olsson, L. & Christakopoulos, P. Lignin boosts the cellulase performance of a GH-61 enzyme from *Sporotrichum thermophile*. *Bioresour. Technol.* **110**, 480–487 (2012).
10. Chylenski, P. *et al.* Enzymatic degradation of sulfite-pulped softwoods and the role of LPMOs. *Biotechnol. Biofuels.* **10**, 177 (2017).
11. Sanhueza, C., Carvajal, G., Soto-Aguilar, J., Lienqueo, M. E. & Salazar, O. The effect of a lytic polysaccharide monooxygenase and a xylanase from *Gloeophyllum trabeum* on the enzymatic hydrolysis of lignocellulosic residues using a commercial cellulase. *Enzyme Microb. Technol.* **113**, 75–82 (2018).
12. Vermaas, J. V., Crowley, M. F., Beckham, G. T. & Payne, C. M. Effects of lytic polysaccharide monooxygenase oxidation on cellulose structure and binding of oxidized cellulose oligomers to cellulases. *J. Phys. Chem. B.* **119**, 6129–6143 (2015).
13. Eibinger, M., Sattelkow, J., Ganner, T., Plank, H. & Nidetzky, B. Single-molecule study of oxidative enzymatic deconstruction of cellulose. *Nat. Commun.* **8**, 894 (2017).
14. Harris, P. V., Xu, F., Kreel, N. E., Kang, C. & Fukuyama, S. New enzyme insights drive advances in commercial ethanol production. *Curr. Opin. Chem. Biol.* **19**, 162–170 (2014).
15. Cannella, D., Hsieh, C. W., Felby, C. & Jorgensen, H. Production and effect of aldonic acids during enzymatic hydrolysis of lignocellulose at high dry matter content. *Biotechnol. Biofuels.* **5**, 26 (2012).
16. Bissaro, B. *et al.* Oxidative cleavage of polysaccharides by monocopper enzymes depends on H<sub>2</sub>O<sub>2</sub>. *Nat. Chem. Biol.* **13**, 1123–1128 (2017).
17. Rieder, L., Stepnov, A. A., Sørlie, M. & Eijsink, V. G. H. Fast and specific peroxygenase reactions catalyzed by fungal mono-copper enzymes. *Biochemistry* **60**, 3633–3643 (2021).
18. Stepnov, A. A. *et al.* The impact of reductants on the catalytic efficiency of a lytic polysaccharide monooxygenase and the special role of dehydroascorbic acid. *FEBS Lett.* **596**, 53–70 (2022).
19. Kuusk, S. *et al.* Kinetics of H<sub>2</sub>O<sub>2</sub>-driven degradation of chitin by a bacterial lytic polysaccharide monooxygenase. *J. Biol. Chem.* **293**, 523–531 (2018).
20. Jones, S. M., Transue, W. J., Meier, K. K., Kelemen, B. & Solomon, E. I. Kinetic analysis of amino acid radicals formed in H<sub>2</sub>O<sub>2</sub>-driven Cu(I) LPMO reoxidation implicates dominant homolytic reactivity. *Proc. Natl. Acad. Sci. U.S.A.* **117**, 11916–11922 (2020).
21. Wilson, R. J., Beezer, A. E. & Mitchell, J. C. A kinetic study of the oxidation of L-ascorbic acid (vitamin C) in solution using an isothermal microcalorimeter. *Thermochim. Acta* **264**, 27–40 (1995).
22. Tulyathan, V., Boulton, R. B. & Singleton, V. L. Oxygen uptake by gallic acid as a model for similar reactions in wines. *J. Agric. Food Chem.* **37**, 844–849 (1989).
23. Kachur, A. V., Koch, C. J. & Biaglow, J. E. Mechanism of copper-catalyzed autoxidation of cysteine. *Free Radic. Res.* **31**, 23–34 (1999).
24. Kittl, R., Kracher, D., Burgstaller, D., Haltrich, D. & Ludwig, R. Production of four *Neurospora crassa* lytic polysaccharide monooxygenases in *Pichia pastoris* monitored by a fluorimetric assay. *Biotechnol. Biofuels.* **5**, 79 (2012).
25. Hegnar, O. A. *et al.* pH-dependent relationship between catalytic activity and hydrogen peroxide production shown via characterization of a lytic polysaccharide monooxygenase from *Gloeophyllum trabeum*. *Appl. Environ. Microbiol.* **85** (2019).
26. Eijsink, V. G. H. *et al.* On the functional characterization of lytic polysaccharide monooxygenases (LPMOs). *Biotechnol. Biofuels.* **12**, 58 (2019).
27. Filandr, F. *et al.* The H<sub>2</sub>O<sub>2</sub>-dependent activity of a fungal lytic polysaccharide monooxygenase investigated with a turbidimetric assay. *Biotechnol. Biofuels.* **13**, 37 (2020).
28. Stepnov, A. A. *et al.* Unraveling the roles of the reductant and free copper ions in LPMO kinetics. *Biotechnol. Biofuels.* **14**, 28 (2021).
29. Bissaro, B., Isaksen, I., Vaaje-Kolstad, G., Eijsink, V. G. H. & Røhr, Å. K. How a lytic polysaccharide monooxygenase binds crystalline chitin. *Biochemistry* **57**, 1893–1906 (2018).
30. Guillen, D., Sanchez, S. & Rodriguez-Sanoja, R. Carbohydrate-binding domains: multiplicity of biological roles. *Appl. Microbiol. Biotechnol.* **85**, 1241–1249 (2010).
31. Forsberg, Z. *et al.* Comparative study of two chitin-active and two cellulose-active AA10-type lytic polysaccharide monooxygenases. *Biochemistry* **53**, 1647–1656 (2014).
32. Crouch, L. I., Labourel, A., Walton, P. H., Davies, G. J. & Gilbert, H. J. The contribution of non-catalytic carbohydrate binding modules to the activity of lytic polysaccharide monooxygenases. *J. Biol. Chem.* **291**, 7439–7449 (2016).
33. Courtade, G., Forsberg, Z., Heggset, E. B., Eijsink, V. G. H. & Aachmann, F. L. The carbohydrate-binding module and linker of a modular lytic polysaccharide monooxygenase promote localized cellulose oxidation. *J. Biol. Chem.* **293**, 13006–13015 (2018).
34. Chalak, A. *et al.* Influence of the carbohydrate-binding module on the activity of a fungal AA9 lytic polysaccharide monooxygenase on cellulosic substrates. *Biotechnol. Biofuels.* **12**, 206 (2019).
35. Forsberg, Z. *et al.* Structural and functional characterization of a conserved pair of bacterial cellulose-oxidizing lytic polysaccharide monooxygenases. *Proc. Natl. Acad. Sci. U.S.A.* **111**, 8446–8451 (2014).
36. Bissaro, B., Kommedal, E., Røhr, Å. K. & Eijsink, V. G. H. Controlled depolymerization of cellulose by light-driven lytic polysaccharide oxygenases. *Nat. Commun.* **11**, 890 (2020).
37. Loose, J. S. M. *et al.* Multipoint precision binding of substrate protects lytic polysaccharide monooxygenases from self-destructive off-pathway processes. *Biochemistry* **57**, 4114–4124 (2018).

38. Wang, B., Wang, Z., Davies, G. J., Walton, P. H. & Rovira, C. Activation of O<sub>2</sub> and H<sub>2</sub>O<sub>2</sub> by lytic polysaccharide monooxygenases. *ACS Catal.* **10**, 12760–12769 (2020).
39. Bissaro, B. *et al.* Molecular mechanism of the chitinolytic peroxygenase reaction. *Proc. Natl. Acad. Sci. U.S.A.* **117**, 1504–1513 (2020).
40. Kuusk, S. & Våljamäe, P. Kinetics of H<sub>2</sub>O<sub>2</sub>-driven catalysis by a lytic polysaccharide monooxygenase from the fungus *Trichoderma reesei*. *J. Biol. Chem.* **297**, 101256 (2021).
41. Li, F. *et al.* A lytic polysaccharide monooxygenase from a white-rot fungus drives the degradation of lignin by a versatile peroxidase. *Appl. Environ. Microbiol.* **85** (2019).
42. Kachur, A. V., Koch, C. J. & Biaglow, J. E. Mechanism of copper-catalyzed oxidation of glutathione. *Free Radic. Res.* **28**, 259–269 (1998).
43. Petrović, D. M. *et al.* Comparison of three seemingly similar lytic polysaccharide monooxygenases from *Neurospora crassa* suggests different roles in plant biomass degradation. *J. Biol. Chem.* **294**, 15068–15081 (2019).
44. Manoil, C. & Beckwith, J. A genetic approach to analyzing membrane protein topology. *Science* **233**, 1403–1408 (1986).
45. Gasteiger, E. *et al.* Protein Identification and analysis tools on the ExPASy Server in *The Proteomics Protocols Handbook* pp. 571–607 (2005).
46. Spezio, M., Wilson, D. B. & Karplus, P. A. Crystal structure of the catalytic domain of a thermophilic endocellulase. *Biochemistry* **32**, 9906–9916 (1993).
47. Østby, H., Jameson, J. K., Costa, T., Eijssink, V. G. H. & Arntzen, M. Ø. Chromatographic analysis of oxidized cello-oligomers generated by lytic polysaccharide monooxygenases using dual electrolytic eluent generation. *J. Chromatogr. A.* **1662**, 462691 (2022).
48. Zamocky, M. *et al.* Cloning, sequence analysis and heterologous expression in *Pichia pastoris* of a gene encoding a thermostable cellobiose dehydrogenase from *Myriococcum thermophilum*. *Protein Expr. Purif.* **59**, 258–265 (2008).
49. Bissaro, B. *et al.* Fueling biomass-degrading oxidative enzymes by light-driven water oxidation. *Green Chem.* **18**, 5357–5366 (2016).

## Acknowledgements

This work was supported by the Research Council of Norway through the OxyMod project (269408) and by the Novo Nordisk Foundation through grant NNF18OC0055736 to Z.F.

## Author contributions

A.A.S. designed experiments, did most of the experimental work, analyzed data and drafted the manuscript. V.G.H.E. and Z.F. provided funding, initiated the research, carried out supervision, helped to design and conduct experiments, interpreted results, and contributed to writing and editing the manuscript.

## Competing interests

The authors declare no competing interests.

## Additional information

**Supplementary Information** The online version contains supplementary material available at <https://doi.org/10.1038/s41598-022-10096-0>.

**Correspondence** and requests for materials should be addressed to V.G.H.E. or Z.F.

**Reprints and permissions information** is available at [www.nature.com/reprints](http://www.nature.com/reprints).

**Publisher's note** Springer Nature remains neutral with regard to jurisdictional claims in published maps and institutional affiliations.



**Open Access** This article is licensed under a Creative Commons Attribution 4.0 International License, which permits use, sharing, adaptation, distribution and reproduction in any medium or format, as long as you give appropriate credit to the original author(s) and the source, provide a link to the Creative Commons licence, and indicate if changes were made. The images or other third party material in this article are included in the article's Creative Commons licence, unless indicated otherwise in a credit line to the material. If material is not included in the article's Creative Commons licence and your intended use is not permitted by statutory regulation or exceeds the permitted use, you will need to obtain permission directly from the copyright holder. To view a copy of this licence, visit <http://creativecommons.org/licenses/by/4.0/>.

© The Author(s) 2022